

Copyright

By

Eric James Heaton

2016

**Paleontological, geochemical, and geophysical climate proxies in Late Pleistocene
lacustrine sediments from Summer Lake, Oregon, western Great Basin**

By

Eric James Heaton, M.S.

**A Thesis Submitted to the Department of Geological Sciences,
California State University Bakersfield**

**In Partial Fulfillment for the Degree of
Masters of Geology**

Spring 2016

**Paleontological, geochemical, and geophysical climate proxies in Late Pleistocene lacustrine
sediments from Summer Lake, Oregon, western Great Basin**

By Eric James Heaton

**This thesis or project has been accepted on behalf of the Department of Geological Sciences
by their supervisory committee:**



Robert Negrini, Ph.D.
Committee Chair

Peter Ernest Wigand
Peter Ernest Wigand (May 25, 2016)

Peter Wigand, Ph.D.
Electronic Signature



Adam Guo, Ph.D.

Acknowledgments

Funding for this project was supported by the National Science Foundation Center for Research Excellence in Science and Technology (CREST) Award #1137774. Funding for the purchase of the UIC Coulometer CM135, Costech 4010 Elemental Analyzer and Malvern Mastersizer 2000 laser particle analyzer was provided by the US Department of Education Award #P031C80013-09.

This work would not be possible without the invaluable guidance and expertise of my advisor, Dr. Robert Negrini, as well as insightful comments from committee advisors, Dr. Peter Wigand and Dr. Adam Guo. A special thanks to Dr. Peter Wigand for his mentoring in palynology. It was a very difficult subject to master and I would have not been able to do it without his help.

Thanks go out to Elizabeth Powers and Sue Holt for their support and putting up with my antics on a daily basis. But of course, mostly provided help with maintaining laboratory instruments and supplies.

Most importantly, my family, friends, and Karol Casas for giving the love and support that has helped keeping me emotionally sane through this whole process. Their support has let me continue with my dreams of Geology. I appreciate their generosity and understanding over all these years.

Abstract:

Paleontological, geochemical, and geophysical data from pluvial Summer Lake, Oregon, western Great Basin are the basis for a high resolution paleoclimate record during a time interval (38-34 ka) including the Mono Lake Excursion, Dansgaard-Oeschger interstadials #8-6, and the end of Heinrich Event 4. The proxies consist of grain-size, C_{org}/N ratio, ostracode faunal counts, and palynology and build on previously-published proxies based on environmental magnetism. Results from granulometry and geochemical analysis and the presence of the ostracode *Cytherissa lacustris* consistently demonstrate the correspondence of low lake conditions and colder water temperatures during Dansgaard-Oeschger stadials, one of which also includes the Mono Lake Excursion found both in the lake and ice core records. Palynological variability seen from *Atriplex*, *Rosaceae*, high spine and low spine *Asteraceae* concentrations, and pollen ratios of *Juniperus/Dip Pinus* and $(Rosaceae+Atriplex+Poaceae+Hi\ Spine+Low\ Spine\ Asteraceae)/(Pinus+Picea+Tsuga\ mertensiana+Sarcobatus)$ suggest warmer/wetter semi-arid woodland conditions during interstadials 8 and 7 and colder/drier continental montane woodland conditions during stadial periods. These results confirm those of earlier studies at Summer Lake and other Great Basin lakes in western North America with respect to the relationship between millennial-scale temperature changes throughout the northern hemisphere and the response of regional climate in western North America at semitropical latitudes. That is, millennial-scale interstadials are associated with warmer, wetter climates in the Great Basin and vice-versa.

Table of Contents

Acknowledgements.....	v
Abstract.....	vi
List of Maps	vix
List of Figures.....	vix
1. Introduction.....	1
1.1 Geological Setting	6
1.2 Age Control	6
2. Methods.....	7
2.1 Core Acquisition and Sampling.....	7
2.2 Ostracode Analysis.....	7
2.3 Magnetic Susceptibility	8
2.4 Carbon and Nitrogen Geochemistry	8
2.5 Grain Size	9

2.6 Pollen Analysis	9
3. Results and Interpretation	11
3.1 Magnetic susceptibility, Mono Lake Excursion Relative Paleointensity Low, and designation of Zones 1-6	11
3.2 Laser Granulometry	12
3.3 Carbon and Nitrogen Analysis	12
3.4 Ostracode Assemblages	13
3.5 Pollen Analysis	15
4. Discussion and Conclusion	17
4.1 North Atlantic temperatures drive climate in the northwestern Great Basin during the Late Pleistocene	17
4.2 Summer Lake paleoclimate record between D-O oscillations #8-6	18
4.3 Climate dipole between Western Great Basin and Northern Sierra Nevada	19
References	28

List of Maps

Map 1	21
Pleistocene Great Basin lake systems	
Map 2	22
Regional map of late Pleistocene Chewaucan Basin	

List of Figures

Figure 1	23
Relative percentage diagram of major pollen, spore and algae from Summer Lake	
Figure 2	24
Principal component analysis of pollen taxa from Summer Lake BB3-I core	
Figure 3	25
Geophysical and geochemical proxies from Summer Lake BB3-I Core	
Figure 4	26
Box and Whisker plot of C_{org}/N ratio by zonation	
Figure 5	27
Summer Lake BB3-I core paleoclimate and lake proxies	

PALEONTOLOGICAL, GEOCHEMICAL, AND GEOPHYSICAL CLIMATE PROXIES IN LATE PLEISTOCENE LACUSTRINE SEDIMENTS FROM SUMMER LAKE, OREGON, WESTERN GREAT BASIN

Eric Heaton

*California State University Bakersfield, Department of Geological Sciences,
9001 Stockdale Highway, Bakersfield, Ca. 93311*

1. Introduction

Summer Lake, Oregon is a subbasin of Pleistocene Lake Chewaucan located in the northwestern-most portion of the Great Basin (Figure 1). Throughout the past 100,000 years, Lake Chewaucan fluctuated over 100 meters in response to regional climate change (Allison, 1982; Cohen et al., 2000; Negrini et al., 2002; Benson, 2004). This is similar to other internally-drained lakes of the northern Great Basin, where the hydrologic systems are especially sensitive to temperature and precipitation related to regional-scale climate fluctuations (Mifflin and Wheat, 1979; Benson et al., 2003). As a result, the lakes within the Great Basin have the potential to accurately record the high frequency, high amplitude climate variations as recognized in lake outcrops, landforms, and sediment cores (Cohen et al., 2000; Negrini et al., 2000; Zic et al., 2002; Reheis et al., 2014). During Marine Isotope Stage 3 (MIS 3), these climate variations may have corresponded to millennial scale climate fluctuations, such as Dansgaard-Oeschger (D-O) and Heinrich events, documented most clearly in Greenland ice cores (Dansgaard et al., 1993; Johnsen et al., 1992; Grootes and Stuiver, 1997; Svensson et al., 2008). It is also suggested from the teleconnected ocean hypothesis that lower/higher temperatures in the North Atlantic region influence lower/higher temperatures in the North Pacific, which, in turn, results in reduced/increased precipitation in the Great Basin (Mikolajewicz et al., 1997; Benson et al., 1997; Hendy and Kennett, 1999).

Benson et al. (1997) used a record from Owens Lake to test the teleconnected ocean hypothesis. Total inorganic carbon (TIC), pollen, and $\delta^{18}\text{O}$ proxies for lake level and hydrological balance were compared with the GISP2 ice core $\delta^{18}\text{O}$ from ~15.8-6.7 ka. The results suggested similar trends in the number, duration, and timing between Holocene dry events at Owens Lake and the recorded cold events in the GISP2 ice core. These results are supported by climate simulations of the Holocene Younger Dryas event (Mikolajewicz et al., 1997). This study suggested colder climate in the North Atlantic Ocean leads to colder climate in the North Pacific Ocean, resulting in drier conditions in Western North America. This suggests that the systems are coupled through atmospheric processes (i.e. teleconnected).

Hendy and Kennett (1999) also tested the teleconnected ocean hypothesis from Santa Barbara basin ODP core 893A. They correlated laminated sediments variations and planktonic foraminiferal isotopic and assemblage changes from core 893A with the GISP2 $\delta^{18}\text{O}$ record between 60-25 ka. The foraminiferal $\delta^{18}\text{O}$ sequence exhibits remarkable similarities in magnitude and shape compared to the GISP2 $\delta^{18}\text{O}$, including the very rapid transitions between stadials and interstadials. Their results suggest at least decadal-scale synchronicity in climatic change between North American Pacific ocean surface waters and North Atlantic Greenland ice sheets. Agreeing with the results of Mikolajewicz et al. (1997), they support that the systems must be coupled through atmospheric processes. Furthermore, they suggested that the recorded high-frequency warming overshoots in sea surface temperatures, documented at the beginning of interstadial periods, are best explained by positive feedbacks from atmospheric warming.

The teleconnection hypothesis was also tested by Zic et al. (2002). They used magnetic mineral proxies to suggest that periods of predicted high lake levels at Summer Lake corresponded to high $\delta^{18}\text{O}$ levels in the GISP2 Greenland ice core record. Previous studies, Negrini et al. (2000) and Cohen et al. (2000), found linkage between low magnetite concentrations (low field susceptibility), high values of TOC, high silt/clay ratios, field relations (i.e. interbedded ostracodal, diatomaceous, and sandy muds; oolitic beds, presence of soil horizons, and reworked shells and intraclasts)- all indicating low lake level. Low magnetite concentrations can be indicative of magnetite dilution and/or dissolution from oxidation and decomposition of organic material when the lake level drops (e.g. Snowball, 1993; Negrini et al., 2000; Lanci et al., 2001). Conversely, high magnetite concentrations were associated with laminated, deep-water sediments with low TOC content and ostracode taxa suggestive of low salinity (Cohen et al., 2000; Negrini et al., 2000). The conclusions from Zic et al. (2002) inferred synchronous climate change between the North Atlantic and the Great Basin, supporting the earlier results by Benson et al. (1997).

The teleconnection hypothesis was further invoked by Benson et al. (2011) using a core from Lake Bonneville. This study proposed that shallow, cold lake events occurred when proxies of $\delta^{18}\text{O}$ were low and TIC and calcite weight fraction were high. Paleomagnetic secular variation (PSV) was used for age control, and compared to the GISP2 $\delta^{18}\text{O}$ record indicating a teleconnection between Great Basin and North Atlantic Dansgaard-Oeschger interstadial (IS) events (Benson et al., 2011). An additional study using two cores from Lake Winnemucca and Pyramid Lake showed similar results (Benson et al., 2012). Again, shallow, cold lake events were interpreted to occur when $\delta^{18}\text{O}$ were low and TIC and calcite weight fraction were high. This study was compared with the GISP2 record and

correlates to the Lake Bonneville study (Benson et al., 2012). However, Reheis et al. (2014) revealed that the core records by Benson et al. (2011) and Benson et al. (2012) do not completely match the geological evidence from outcrops of Lake Bonneville. Reheis et al. (2014) noted that the interpreted periods suggested to be indicative of a drop in lake level, conflicts with outcrop interpretations, which indicate that the opposite occurred.

In addition to the tests based on lake core analyses, Denniston et al. (2007) tackled the teleconnection hypothesis using a stalagmite $\delta^{18}\text{O}$ record from Goshute Cave in the Great Basin. A comparison to the GISP2 ice core denoted similar timing and structure to D-O events 23-21, providing further evidence of synchronous climate fluctuations between the North Atlantic and Great Basin, North America. However, they make note that the temperature and precipitation moisture sources denoting the values of $\delta^{18}\text{O}$ from the speleothems is unclear and could be of importance in the interpretation.

Another stalagmite study from McLean's Cave, Central California Sierra Nevada foothills suggests a correlation between D-O events and central California climate conditions that were drier and warmer during interstadials (Oster et al., 2014). During the interval containing interstadials #15-18, increased levels of $\delta^{18}\text{O}$, $\delta^{13}\text{C}$, reflectance (suggests decreases in growth rate), and trace element concentrations, as well as decreases in $^{87}\text{Sr}/^{86}\text{Sr}$, denote changes in climate from colder/wetter stadial times to warmer/drier interstadials. Contrasting with the results from the stalagmite, however, Great Basin lake cores suggest a warmer/*wetter* climate during interstadials at Summer Lake. For example, Cohen et al. (2000) suggests that lake levels at Summer Lake are inversely linked with TOC and salinity, the latter of which was inferred from ostracode taxonomy. Based on these proxies, lake level

high stands show periods of low depositional energy, fresher water, and increased discharge, and vice versa

In order to reconcile the discrepancy between the studies of lake cores and the stalagmite study, we present a high resolution climate record for Summer Lake during the MLE and from D-O events 8-6. Paleontological, geochemical, and geophysical proxies of granulometry, TIC, organic carbon/nitrogen ratio (C_{org}/N), ostracode taxonomy, and palynology are used to suggest climate fluctuations with regard to lake temperature, precipitation, and lake level.

The specific goal of this study is to test the hypothesis of Benson et al. (1997) and Zic et al. (2002) that Great Basin lakes, including Summer Lake, respond to hemispheric-scale D-O oscillations by becoming shallow during cold intervals, and vice versa. Building on the prior results of Zic et al. (2002), more recent work at Summer Lake has uncovered a full vector component record of the 35-32 ka Mono Lake geomagnetic excursion in the BB3-I depocenter core (Map 1) from Summer Lake, including its characteristic paleointensity low (Negrini et al., 2014 and references therein). These excursions are large-scale fluctuations in the direction and intensity of Earth's magnetic field and may represent aborted magnetic reversals, short-duration complete reversals, and/or large-scale secular variation (Laj and Channell, 2007). The interval of lowest intensity within the Mono Lake Excursion (MLE) is recorded as a spike of high concentration of the ^{36}Cl radioisotope in the Summit GRIP ice core during the cold, stadial interval immediately above IS 7 (Wagner et al., 2000) and starting at 34.8 ka on the GICC05 age scale (Svensson et al., 2008). This low intensity feature is thus used as a chronostratigraphic tie point between the ice core and BB3-I Summer Lake climate records.

1.1 Geologic Setting

Summer Lake, Oregon is located in a subbasin of Pleistocene pluvial Lake Chewaucan near the northwestern margin of the Great Basin (Map 2). It has the lowest bottom elevation of the subbasins of Lake Chewaucan (Allison, 1982). Prior to the most recent pluvial maximum, the Chewaucan River fed the Summer Lake subbasin. This basin was internally-drained with large sources of water from rain and glacier melt (Benson et al., 2003), and possibly from groundwater flow from adjacent basins (Allison, 1982). At its maximum, Lake Chewaucan was 114 m deep and covered 1244 km² (Allison, 1982). The Chewaucan basin formed from a complex down-dropped fault block between Winter Ridge and Albert Rim (Allison, 1982). Summer Lake lies on the western rim of a north-south trending half-graben, tilted to the west (Donath, 1962; Walker, 1969; Baldwin, 1981). The source rock is principally volcanic in origin, mostly basalt with some rhyolite and dacite flows, and highly faulted tuffaceous rocks (Allison, 1982; Walker and MacLeod, 1991).

1.2 Age Control

Radiocarbon dates and tephrochronology of layers above the MLE and below Heinrich event 4 were first documented in a core from the Summer Lake depocenter by Zic et al. (2002). New studies from the core of this study (BB3-I) have undertaken a more detailed examination of the rock magnetic properties, providing improvements in age control of the Wono tephra (34-30 cal ka B.P.), Tephra G, and Mount St. Helens Cy (47-43 cal ka B.P.) found between 9.23 and 13.7 mbgs (Negrini et al., 2000; McCuan, 2011; Benson et al., 2012; Kuehn and Negrini, 2012; Negrini et al., 2014). The age of the Wono tephra, located at 9.23 mbgs, was calculated by averaging two bracketing radiocarbon dates, resulting in an age estimate of 29.7±510 ¹⁴C kyr B.P. (McCuan, 2011; Negrini et al., 2014). Additionally,

Benson et al. (2012) provided consistent age control from ^{14}C and PSV correlations of marine sediments that are indirectly tied to the North Atlantic millennial scale climate fluctuations.

An additional twelve AMS radiocarbon dates were obtained within and below the Wono tephra in the BB3-I core, extending below the Heinrich event 4 unconformity (McCuan, 2011; Negrini et al., 2014). A lake reservoir effect conservatively estimated at 500 years was subtracted from the raw ^{14}C before calibration, which suggests that the resulting ages were maximal (Negrini et al., 2014).

2. Methods

2.1 Core Acquisition and Sampling

The BB3-I core was obtained from Summer Lake, Oregon in September 2010 using a modified Livingston piston coring device (McCuan, 2011). The ~14 m deep, 11 cm diameter core was obtained only tens of meters from the location of the 1992 BB1 core site at 42.8057° N, 120.7831° W (McCuan, 2011). The core was split in half with a wire with each half being used for sampling and analysis. Sedimentary layers associated with the intact core extended without deformation to the outside of the core. The MLE is found between 9.4 – 11 mbgs of the BB3-I core (Negrini et al., 2014). Two 5-cm³ samples were taken continuously between 12.60-9.94 mbgs for a total of 178 samples. One set of samples was analyzed for ostracodes and the other for grain size and carbon geochemistry. Fifty-one additional 5 cm³ samples were taken in 1 cm slices across the core in 5 cm intervals between depths 10.5-13 mbgs for pollen analysis. All samples were taken away from the margins of the core with a flanged sampling device to prevent compression and sediment mixing.

2.2 Ostracode Analysis

Methods for ostracode preparation and analysis were adapted from Palacios-Fest et al. (1993). Samples were disaggregated with boiling water and hexametaphosphate and required to sit at room temperature for 48 hours, stirring once daily. The samples were then rinsed using a washing lid and a 63 μm , 8-inch sieve, to remove the fine-grained sediments and preserve the coarse grains and biomass. The samples were left to dry, and the mass of the dry sediment was recorded before and after the ostracodes were extracted. All of the samples were then analyzed through binocular microscopes, and the ostracode species were identified and counted.

2.3 Magnetic Susceptibility

The magnetic susceptibilities were measured using a Bartington MS2/MS2B meter/sensor combination. The samples were measured in centimeter-gram-second (CGS) with a 1.0 meter sensitivity setting and then converted to (SI) units. Mass-normalized values calculated from these values and are reported here as kg^{-1} .

2.4 Carbon and Nitrogen Geochemistry

Methods for carbon and nitrogen geochemistry preparation and analysis were modified after Blunt and Negrini (2015). Sample splits were placed in an oven at 105°C for 24 hours, then crushed with a mortar and pestle, and left to cool in a desiccator for a minimum of an hour. TIC was analyzed by putting 100 mg of dried, cooled sediment in a silicone cup and placing it in the UIC CM135 coulometer after CO₂ was forced in a UIC CM5230 Acidification Module. A CaCO₃ standard of 19-20 mg was analyzed before samples were run and was used to correct sample measurements. A Costech 4010 Elemental Analyzer was used to determine total carbon and nitrogen. 20-25 mg samples of crushed, dried sediment were measured and placed in tin cups and compressed to remove air. Two

runs with atropine, two blanks, and three standards of atropine were used to calibrate the machine before the samples were combusted and measured for total carbon and nitrogen. TOC was calculated using the difference between total carbon (TC) and TIC (Meyers and Doose, 1999). C_{org}/N ratios were determined using TOC and nitrogen results after they were converted to molar percentages.

2.5 Grain Size

The other half of the 2 cm split was mixed with deionized water and dried in the oven. One gram of dried sediment was mixed into 10 ml of deionized water and 5 ml of hexametaphosphate and required to sit at least 24 hours before use in the Malvern Mastersizer 2000 laser particle analyzer. The samples were wet-sieved using a 16 mesh-size sieve to prevent any grains larger than 1 mm from entering the particle analyzer. Larger grains were archived. The sieved samples were then split into aliquots up to 1/16 of the original sample size using a Humboldt splitter, allowing for custom sample sizes submitted to the particle analyzer to attain ideal laser obscuration (Sperazza et al., 2004). The mean is reported as bulk grain size in microns.

2.6 Pollen Analysis

Methods for pollen extraction were adapted from the swirl technique (Hunt, 1985). 2.5 cm³ of each sample were transferred to a beaker and covered with deionized water to help separate detrital grains. Two lycopodium tracer tablets (batch #124961) were added to each sample, stirred using a swirl technique, and allowed to rest to separate silt and clays from larger grains. The silt and clay separates were then poured into test tubes and centrifuged to separate clays. The liquid was decanted and the process was repeated until all silts were transferred to fill test tubes. The silt-rich samples were then vortexed, centrifuged, and

decanted with boiling water repeatedly until water was clear and fine grained clays were removed.

Heavy liquid separation using polysodium tungstate (polygee) was prepared to a specific gravity of 2.2 to create needed pollen float. The samples were vortex-mixed, filled with polygee, and centrifuged. The pollen float was placed into a new test tube and concentrated by centrifuging with boiling water. The sample was then treated with boiling water and centrifuged to remove any remaining clays and polygee. Safranin stain was added and the samples were washed with ETOH, vortexed, centrifuged, and repeated with no stain. The samples were treated with tert-butyl alcohol, vortexed, centrifuged, decanted, and poured into a 2 ml vial. 2000cs silicon oil was added to the vials until an approximate ratio of 1/3 sample, 1/3 tert-butyl, and 1/3 silicon oil was achieved. The vials were thoroughly vortex-mixed and left to sit out for at least 24 hours to allow the alcohol to completely evaporate. The samples were mixed thoroughly, mounted to a slide, and sealed with nail polish.

Pollen was counted using 400X magnification with a minimum of 300 counts per slide. Pollen, spores, and algae were classified to the lowest taxonomic level possible using reference material from the UNR Geography Palynology Lab, the CSUB CREST Lab, and from published reference keys (Moore and Webb, 1978; Kapp et al., 2000). Pollen of *Cupressaceae* and *Taxaceae* appearance have been assigned to *Juniperus*, the dominant native taxa in the region.

The microfossil record was separated into relative percentage categories constituting terrestrial pollen, aquatic pollen, spores, and algae (Figure 1). Terrestrial pollen percentages were calculated from the sum of terrestrial pollen, excluding *Pinus*. *Cyperaceae* constitutes nearly 100% of the aquatic pollen record. As a result, aquatic pollen percentages were

calculated from the sum of all pollen, including terrestrial pollen, so that changes in *Cyperaceae* abundances are apparent. Spore percentages were calculated independently upon only individual spore counts. Algae was calculated similarly.

Several pollen taxa (*Juniperus* (juniper), *Rosaceae* (roses), *Atriplex* (shadscale), *Poaceae* (grasses), High Spine Asteraceae (aster-type sunflowers), Low Spine Asteraceae (ragweed-type sunflowers), *Dip Pinus* (yellow pine types), *Picea* (spruce), *T. mertensiana* (mountain hemlock), *Sarcobatus* (greasewood)) serve as proxies for changes in climate conditions within the Great Basin (Thompson et al., 1999; Cohen et al., 2000; Wigand and Rhode, 2002). The correlations of these pollen types can be seen as a biplot of Principal Components 1 and 2 (Figure 2). Pollen ratios of *Juniperus/Dip Pinus* and $(Rosaceae+Atriplex+Poaceae+High\ Spine+Low\ Spine)/(Dip\ Pinus+Picea+T. mertensiana+Sarcobatus)$ [shrub/cold conifer index] were thus calculated (Figure 5) using different clusters from the Principal Component analysis to indicate changes in climate.

3. Results and Interpretation

3.1 Magnetic susceptibility, MLE Relative Paleointensity Low, and designation of Zones 1-6

Values of low-field magnetic susceptibility (κg^{-1}) range between 0.026-0.115 κg^{-1} within this study (Figure 3A). Six zones are identified based on magnetic susceptibility trends. These fluctuate between two zone types characterized as relative highs and lows, with higher values in Zones 2, 4, and 6. Consistent with the results of Zic et al. (2002) and Negrini et al. (2014), higher values of magnetic susceptibility are taken as suggestive of deeper lake periods based on the observations presented in previous sections. With the presence of the low paleointensity feature of the Mono Lake geomagnetic excursion in both the Summer Lake sediments and the GRIP ice core, Zones 2, 4, and 6 are correlated with

GICC05 interstadials #8, #7, and #6, respectively (Wagner et al., 2000; Zic et al., 2002; Svensson et al., 2008; Negrini et al., 2014). More specifically, the low intensity part of the MLE occurs in the BB3-I sediments within BB3-I Zone 5 (i.e., between IS#s 7 and 6) at 10.9-10.6 mbgs (Negrini et al., 2014). This interval corresponds with the high concentration of ^{36}Cl found within the GRIP ice core during the stadial interval between IS#s 7 and 6, as defined by the $\delta^{18}\text{O}$ record of the ice core (Wagner et al., 2000; Svensson et al., 2008). Thus, Zones 1, 3, and 5 are interpreted as stadial periods of D-O events.

3.2 Laser Granulometry

The sediments of BB3-I within the studied interval are very fine-grained silts and clays, consistent with a lake depocenter environment. Mean bulk grain size of the interval study is 9.9 μm and ranges from 3-29 μm with a standard deviation of 3.2 μm (Figure 3B). Zones 1, 3, 5, and 6 are characterized by relatively high bulk grain sizes with averages of 10.3, 10.14, 10.07, and 13.05 μm , respectively, whereas Zones 2 and 4 are characterized by relatively low bulk grain sizes with averages of 8.69 and 9.86 μm , respectively. Zones 4 and 6 consist of grain size spikes of 29.23 and 22.69 μm , respectively, which skew mean grain size values positively.

Zone 6 is interpreted to be IS #6 from high magnetic susceptibility values. Interstadial 6 is considerably shorter than either IS #8 or #7 in both the NGRIP ice core Summer Lake sediment records. This may suggest a short-lived interstadial period in which lake size did not have enough time to grow larger and become deeper; thus the interpretation why grain size is high during this period. This is explained in detail at the end of the results and interpretation section.

3.3 Carbon and Nitrogen Analysis

TIC remained consistently low throughout the core with a mean of 0.3%, and only three samples yielded values greater than 1% (Figure 3C). These values are within the level of experimental noise (Kirby et al., 2012). TOC values were significantly higher than TIC, ranging up to 3.1%, although still with a low mean of 1.1% (Figure 3D). The TOC signal is mirrored almost exactly by variations in N% (Figure 3E), suggesting that this combined signal reflects varying organic productivity over time. Total organic Carbon to Nitrogen ratio (C_{org}/N) values range between 1 and 170, averaging 28 (Figure 3F). Box and Whisker plots of C_{org}/N based on averages from each zone, exhibit the fluctuation between two zone types characterized by relative highs and lows. Zones 1, 3, 5, and 6 are characterized by relatively low C_{org}/N values, while Zones 2 and 4 are characterized by relatively high C_{org}/N (Figure 4).

Lacustrine C_{org}/N has been used as a proxy for increased discharge during intervals of wetter climate and deeper lake levels (Meyers and Ishiwatari, 1993; Kirby et al., 2012; Blunt and Negrini, 2015). C_{org}/N values are affected by the amount of cellulose in organic matter of a plant; i.e., vascular (cellulose) terrestrial plants have higher values of C_{org}/N than nonvascular aquatic plants (Meyers and Ishiwatari, 1993). Hence, higher values of C_{org}/N are interpreted to be related to increased transport of terrestrial organic material by increased precipitation and runoff (Kirby et al., 2012; Blunt and Negrini, 2015).

3.4 Ostracode Assemblages

L. ceriotuberosa was abundant and continuous throughout the BB3-I core, with a total of 7862 ostracode count values. *C. lacustris* was found exclusively in Zones 2, 3, and 5 at intervals of 12.58, 11.86 – 11.49, and 11.01 – 10.5 mbgs, respectively, and with a total of 468 ostracode count values. Of importance, *C. lacustris* found in Zone 2 at 12.58 mbgs may be

present in this interval instead of Zone 1 due to reworked sediment from the 5,000-year unconformity at 12.60 mbgs (Negrini et al., 2014). A rapid drop in radiocarbon ages across this boundary and the fact that the 40 Ka Laschamp Excursion is missing suggest this unconformity to be either nondepositional, due to the erosion of several thousand years of sediments, or a combination of both processes from ~42 to ~37 ka of the BB3-I core (Negrini et al., 2014). Single counts of *L. bradburyi* and *L. sappaensis* occur simultaneously at 10.83 mbgs with additional single counts of *L. bradburyi* found at 11.07 mbgs and 11.99 mbgs. One count of *C. vidua* was found at 10.91 mbgs.

C. lacustris is a limnetic, stenotopic species that is restricted to low temperatures (less than 19°C) and low salinities (10-1,000 mgL⁻¹ TDS) (Palacios-Fest et al., 1993; Delorme, 1969; Bunbury and Gajewski, 2009). The species has been long known as a deep, cold-water indicator present in Lakes Baikal and Hovsogul in Russia and Lake Biwa in Japan (Smith and Janz, 2008). In the Pleistocene, it has been documented from Lake Chewaucan (Summer Lake), Oregon (Palacios-Fest et al., 1993), Lake Bonneville, Utah (Lister, 1975; Oviatt et al., 1999; Balch et al., 2005), and Lake Geneva, Switzerland (Decrouy et al., 2012). However, Bunbury and Gajewski (2009) reported its existence in shallow, cold water wetlands and thirteen other lakes in the Canadian Arctic Circle. According to these authors, *C. Lacustris* can tolerate elevated sulphate values, but prefers sites with low ion concentration, i.e., fresher waters.

Limnocythere ceriotuberosa, the most prominent and continuous species found in the BB3-I core, lives in a wide range of alkaline-rich water, but no Cl⁻ or SO₄²⁻-rich systems (Forester, 1986). This eurytopic taxon tolerates a wide range of salinity (5000-25000 mgL⁻¹ TDS) and temperature (4-32°C) (Bachhubber and Catto, 2000). Balch et al. (2005) indicate

that dominance of this species in lakes results from increasing fluvial input that favors an increasing alkalinity/Ca ratio. Ubiquitous, the species is abundant in the geologic record across western North America, including Summer Lake, Oregon; Owens Lake, California; Great Salt Lake, Utah; and Lake Estancia, New Mexico, among others (Palacios-Fest et al., 1993; Carter, 1997; Balch et al., 2005; Bachhubber and Catto, 2000).

3.5 Pollen Analysis

Pinus dominates the record and constitutes between 30 to 93 percent of the total terrestrial pollen. Other major contributors of terrestrial pollen consist of *Picea*, *Abies*, *Juniperus*, *Artemisia* (sagebrush), *Atriplex*, high spine *Asteraceae*, and *Rosaceae*. These mostly contain single counts of *Tsuga mertensiana*, *Tsuga heterophylla* (western hemlock), *Pseudotsuga* (Douglas fir), *Salix* (willow), *Allium* (onion), *Phlox*, *Alnus* (alder), *Lillaceae* (lily), *Eriogonum* (buckwheat), *Ephedra* (Mormon tea), *Quercus* (oak), *Poaceae*, low spine *Asteraceae*, and *Sarcobatus*. *Cyperaceae* (sedges) is almost completely continuous and dominates the aquatic pollen record with single counts of *Typha latifolia* (wide-leafed cat-tail) and *Typha sparganium* (narrow-leafed cat-tail). Spores consist of single counts of *Botrychium*, *Selaginella*, *Lycopodium*, *Pteridium*, *Trite spores*, *Athyrium*, and *Bryophyta*. *Botryococcus* dominates the algae record in both percentages and individual counts.

Additional counts of algae, *Pediastrum boryanum*, *P. kawraiskyi*, and *P. simplex* are present within the cored interval. Algae are more or less randomly distributed with respect to depth.

The pollen record is comprised of two characteristic pollen assemblages for all 6 zones. Zones 1, 3, 5, and 6 consist of relatively high dominance of total *Pinus* (72-93%) and are nearly devoid of *Atriplex*, high spine, low spine, and *Cyperaceae*. This is supplemented with the inclusion of the salt-tolerant desert shrub *Sarcobatus* (Cohen et al., 2000; Donovan

et al., 1996), suggesting the possibility of drier conditions, but also of seasonally higher ground water bringing salts upward in the soil profile. Zones 2 and 4 are characterized by strong decreases in total *Pinus* percentages and strong increases in *Atriplex*, high spine *Asteraceae*, *Cyperaceae*, and *Poaceae*, as well as the inclusion of low spine.

High spine and low spine are most likely *Chrysothamnus* (rabbit brush) and *Ambrosia*, respectively, which are common today within the Chewaucan Basin (Cohen et al., 2000; Wigand and Rhode, 2002) and indicate increases in summer precipitation (Thompson et al., 1999; Wigand and Rhode, 2002). Similarly, *Poaceae* is suggestive of wetter conditions (Cohen et al., 2000; Wigand and Rhode, 2002). These pollen taxons, coupled with the desert scrub *Atriplex* (Thompson et al., 1999; Wigand and Rhode, 2002), could suggest warmer and wetter conditions during Zones 2 and 4.

The Dip *Pinus* record is dominated by a relatively small *Pinus* diploxylon-type, interpreted to be *Pinus contorta*. This taxon has an affinity for colder/drier climate conditions (Thompson et al., 1999), and is prevalent at Summer Lake both today and in the past (Cohen et al., 2000). The dominance of *Pinus contorta* coupled with colder and drier taxons of *Picea*, *T. mertensiana*, and *Sarcobatus* suggests the ratio of $(Rosaceae+Atriplex+Poaceae+High\ Spine+Low\ Spine)/(Dip\ Pinus+Picea+T. mertensiana+Sarcobatus)$ [cold conifer/shrub index] may indicate warmer and wetter conditions during periods of greater *Rosaceae*, *Atriplex*, *Poaceae*, High Spine, and Low Spine concentrations (Zones 2 and 4). Additionally, the ratio of *Juniperus/Dip Pinus* shows a similar trend suggesting that *Juniperus* was more prevalent during periods of increased precipitation. This may indicate the presence and dominance of the semiarid woodland *Juniperus occidentalis* during interstadials and the continental montane woodland *Pinus*

contorta during stadials (Thompson et al., 1999; Cohen et al., 2000; Wigand and Rhode, 2002). This is similar to other research done at Summer Lake and surrounding Great Basin regions that infer a distinction between a semiarid woodland versus continental montane woodland during different climate regimes (Wigand and Rhode, 2002; Cohen et al., 2000).

Zone 6 (IS 6) shows increases in the *Juniper/Dip Pinus* ratio and suggests a warmer/wetter climate; however, additional proxies do not demonstrate comparative warmer/wetter climate, deeper lake level, or increases in discharge during other D-O Interstadial periods. Interstadial 6 is considerably shorter than either IS #8 or #7 in both the NGRIP ice core Summer Lake sediment records. This may suggest a short-lived interstadial period in which: 1) indicative plant species did not have enough time to migrate and flourish to record increases in indicative pollens or C_{org}/N ratio, and 2) lake size did not have enough time to increase comparably to record significant grainsize changes.

4. Discussion and Conclusion

4.1 North Atlantic temperatures drive climate in the northwestern Great Basin during the late Pleistocene

Working on an adjacent core from the same lake as this study, Zic et al. (2002) supported the teleconnection hypothesis (e.g., Hendy and Kennett, 1999) suggesting that temperature changes in the NE Pacific Ocean responded on a decadal or sooner scale, the classic millennial-scale changes in the North Pacific region via rapid atmospheric circulation processes. Warmer/cooler temperatures in the NE Pacific then were hypothesized to increase/decrease precipitation in the Great Basin due to increased evapotranspiration (e.g., Benson et al., 1997). In the Zic et al. (2002) study, age control was based on radiocarbon dating and tephrochronology, which had sufficient resolution to identify the D-O oscillations

in lake-level corresponding to the Bond cycle between Heinrich Events #4 and #3.

Radiocarbon dates in this age range do not have the necessary resolution to distinguish between interstadial and stadial halves of the individual D-O events. However, Zic et al. (2002) were able to demonstrate a distinctive correspondence between a low Summer Lake interval and the cold North Atlantic stadial interval between IS #7 and #6 due to the observation that both the Summer Lake sediments and the Greenland ice core contained records of the Mono Lake excursion low intensity/inclination interval within this interval. This observation locked the phases of the D-O oscillations between the Greenland ice core temperature and Great Basin lake level records. The Mono Lake excursion record was later reproduced in greater detail in the core of this present study by Negrini et al. (2014). These newer results supported the Zic et al. (2002) D-O phase lock, with an estimate of paleointensity of the Mono Lake excursion from the Great Basin thereby allowing a direct comparison of paleointensities between the Great Basin lake sediments and the ice core. The present study presents new proxies of lake level and temperature to supplement the Zic et al. (2002) lake level proxies based only on environmental magnetism.

4.2 Summer Lake paleoclimate record between D-O oscillations #8-6

Varying terrestrial climate conditions are concluded from pollen and pollen ratios. Increases in *Atriplex*, *Poaceae*, *Rosaceae*, high spine and low spine pollens and ratios of *Juniperus/Dip Pinus* and the shrub/cold conifer index collectively support a warmer/wetter semiarid woodland regional climate during IS #8 and #7. This is coupled with increases in C_{org}/N ratio and smaller grain size, indicating increased lake discharge and deeper lake levels as shown in Figure 5. The opposite holds true during stadial periods, including the one between IS #7 and #6 that contains the intensity low of the Mono Lake excursion, which

show absences in *Atriplex*, high spine and low spine, decreases in *Rosaceae*, and decreases in pollen ratios indicating colder/drier continental montane regional climate conditions. This set of observations is coupled with decreases in C_{org}/N ratio and larger grain size, indicating decreased lake discharge and shallower lake levels. The intervals predicted to be deposited during stadials also contain the cold water ostracode *C. lacustris*, strongly suggesting that these zones were deposited when lake temperature were significantly lower.

In summation, this study suggests deeper, warmer waters at times of D-O interstadials, which is consistent with results from other western North American lakes (Benson et al., 1997; Zic et al., 2002; Benson et al., 2011; Benson et al., 2012). Overall, these results collectively support the warmer/*wetter* and colder/*drier* hypothesis for the western North American response to hemispheric, millennial-scale climate change during MIS 3.

4.3 Climate dipole between Western Great Basin and Northern Sierra Nevada

This study may provide additional evidence of a climate dipole between Western Great Basin and Northern Sierra Nevada, as suggested by Wise (2010) for historic times, Mensing et al. (2013) during the Late Holocene and Oster et al. (2015) during the Last Glacial Maximum, and from the otherwise contrary results (drier and warmer climate during IS #15-18) suggested by Oster et al. (2014).

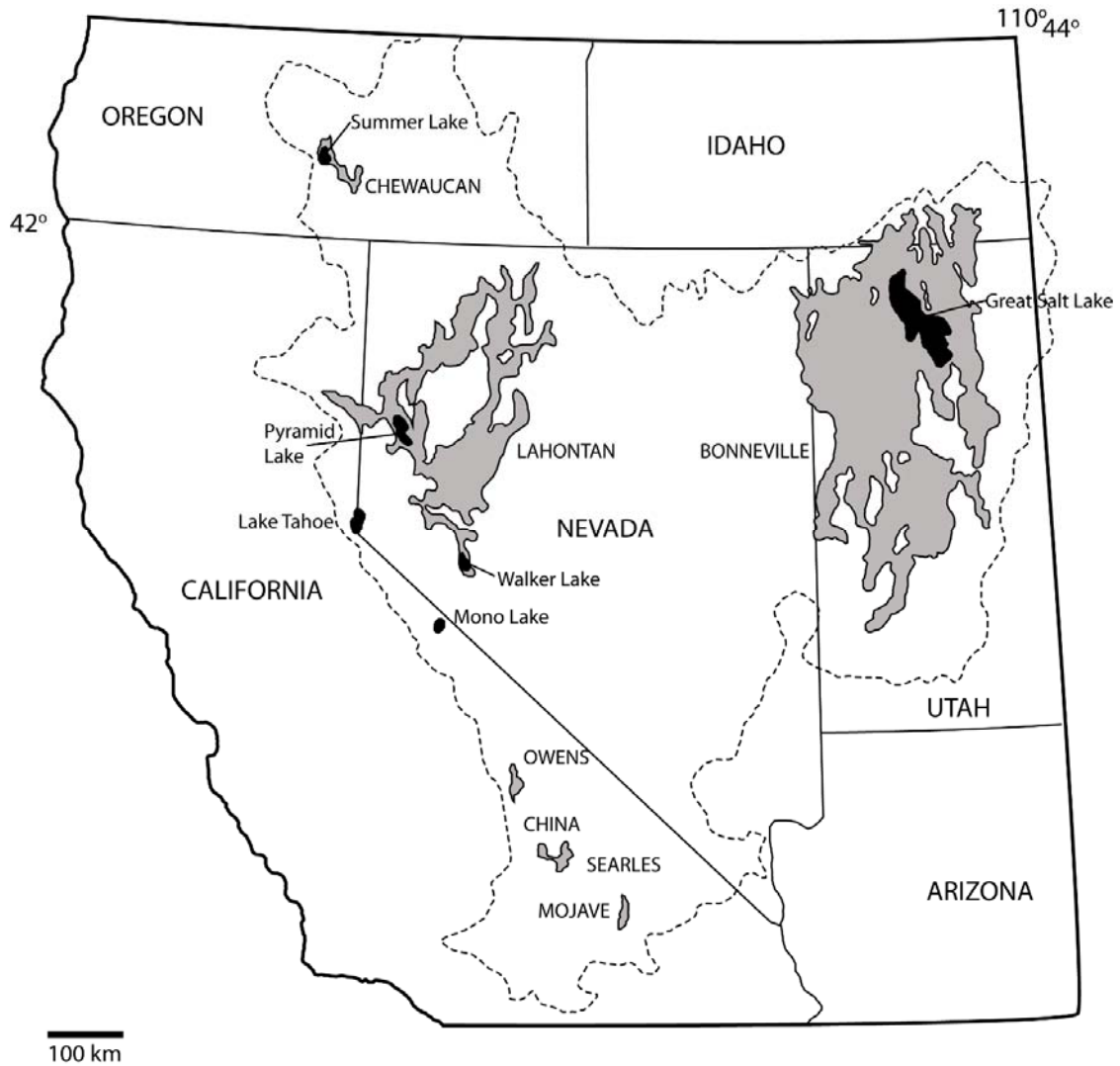
Wise (2010) generated climate models of El Niño-related hydroclimate variability from north-south dipole precipitation anomalies in the western United States suggesting a north-south trending transition boundary located within a latitudinal zone of 40–42°N, comprising parts of eastern Washington, eastern Oregon (including Summer Lake), and western Colorado. Mensing et al. (2013) suggested a similar north-south trending dipole

boundary between 40–42°N during the termed Late Holocene Dry Period (2800-1850 cal yr BP). Their core record from Stonehouse Meadow contains diatom, sedimentary, mollusk and pollen evidence suggesting an extended dry period from ~2800 to 1850 cal yr BP.

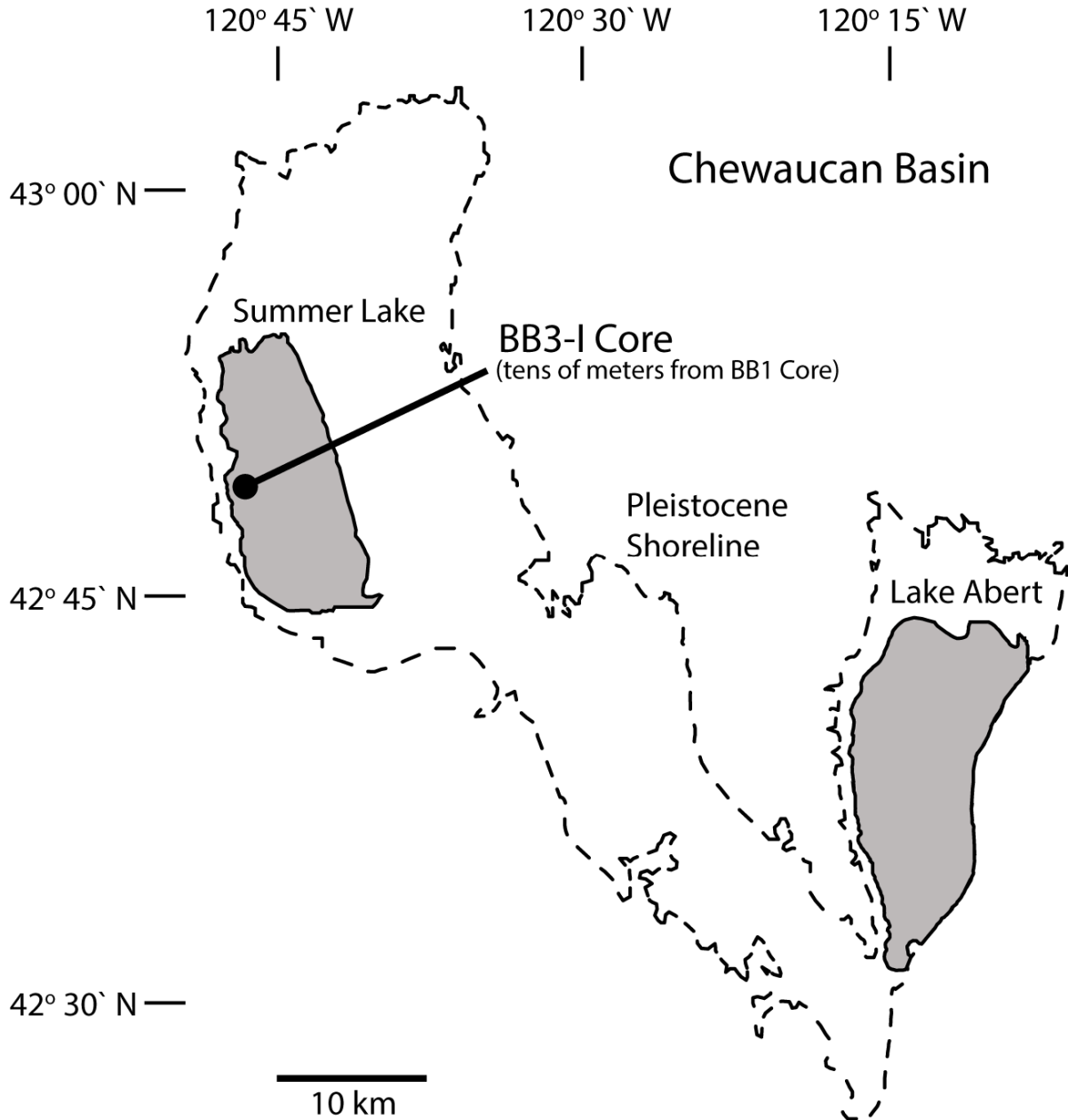
Comparison of their record with additional multi-proxy records across the Great Basin suggests that this dry period was regional. Yet, northern Great Basin studies either indicate no discernable evidence of drought or suggest wetter conditions during this period of time (Mensing et al., 2013).

Oster et al. (2015) proposed an analogous climate dipole from climate simulations, suggesting a northwest-southeast trending paleodipole transition zone between 31.3-47.61°N during the Last Glacial Maximum. In this study, they assembled a collection of precipitation proxy reconstructions from lakes, speleothems, groundwater deposits, packrat middens, and glaciers and compared them with climate simulations to determine the drivers of hydroclimatic fluctuations in western North America. From these data, it was concluded that a stronger jet stream controlled by high-pressure systems best represents the regional hydroclimate fluctuations during the Last Glacial Maximum. More specifically, a wetter regional hydroclimate apparently occurred south of the transition zone, and drier conditions north of the zone, closer to the ice sheet.

Thus, at least between historic times and the Last Glacial Maximum, several studies have suggested various occurrences of a climate dipole in the western United States. With the suggested warmer/wetter conditions seen at Summer Lake during IS #7 and #8 and warmer/drier conditions seen at McLean's Cave (central California) during IS #15-18 (Oster et al., 2014), it is not unreasonable to assume the possibility of a similar paleodipole during D-O oscillations.



Map 1. Map of the extent of Great Basin lake systems (dashed line). Major Pleistocene lakes are denoted in gray and modern remnants in black. The location of Summer Lake is on the westernmost edge of the Great Basin (after Benson, et al., 2012).



Map 2. A detailed map of the Chewaucan Basin with the modern lakes denoted in gray. The ancient Pleistocene high stand shoreline is denoted with a dashed line. Summer Lake lays on the western edge of the Chewaucan Basin with the BB3-I core denoted on the western edge of the lake. This core was taken tens of meters from the original 1992 BB1 core.

Relative Percentage Diagram of Major Pollen, Spores and Algae from Summer Lake BB3-I Core

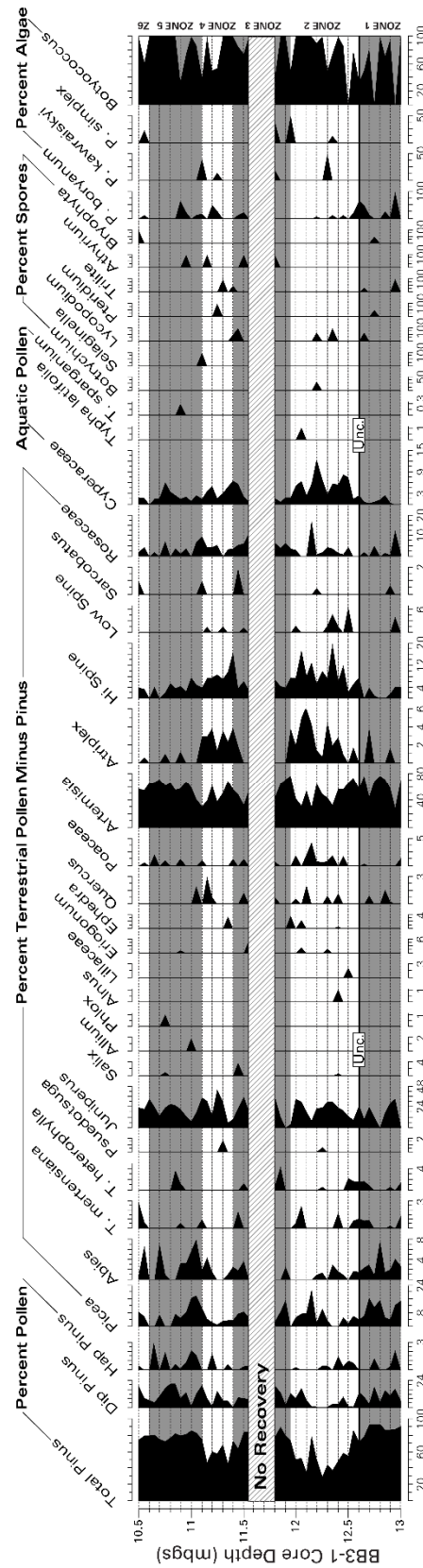


Figure 1. Relative percentage diagram of major pollen, spore and algae types shown stratigraphically from the BB3-I core from 10.5-13 mbgs. Blue backgrounds correspond to colder/drier climate while white backgrounds correspond to warmer/wetter climate.

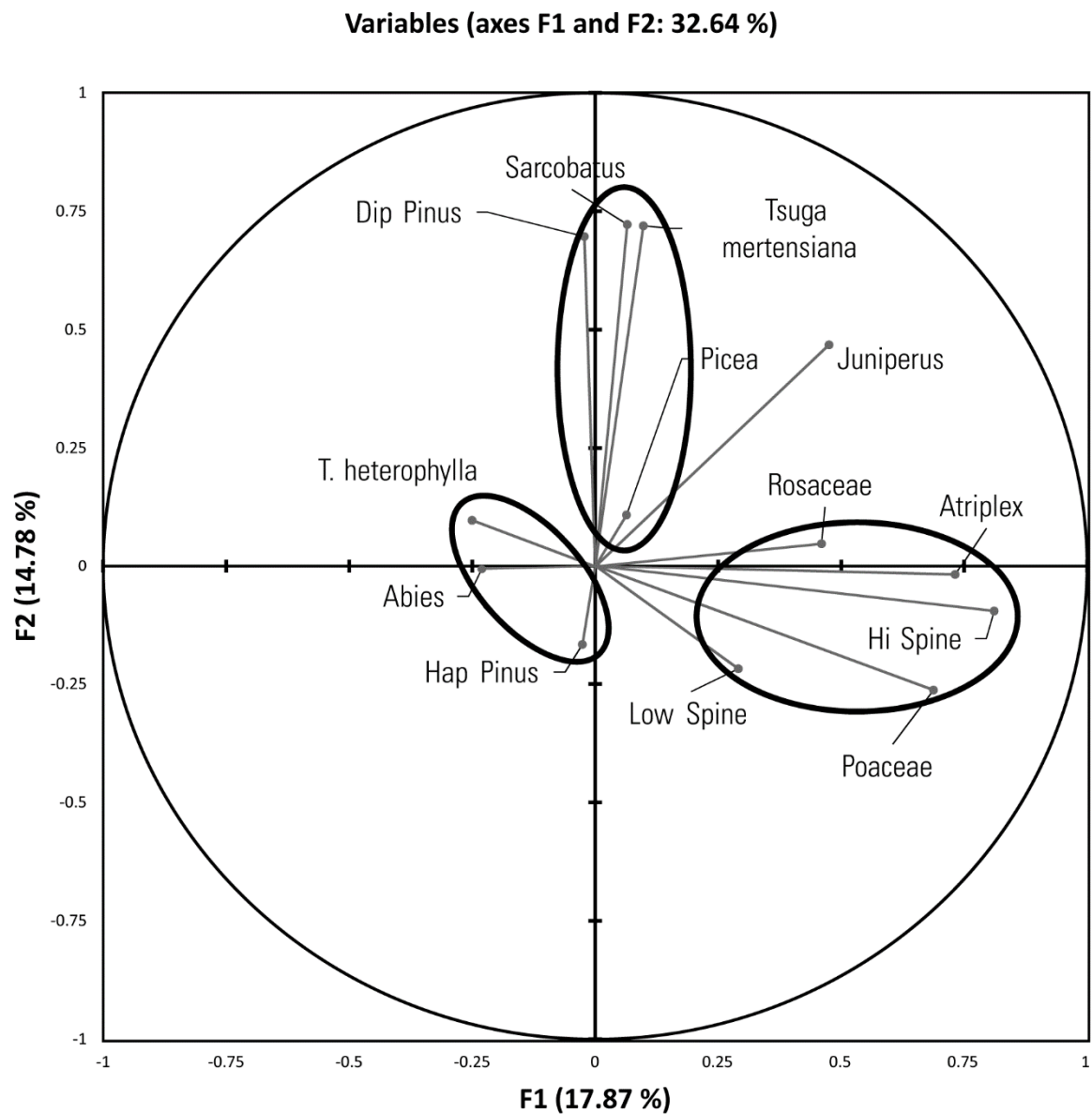


Figure 2. Principal components analysis biplot for BB3-I core showing clusters (circles) of eigenvectors (arrows) of each taxon. Taxons are interpreted to have significance reflecting changes in regional temperature and precipitation.

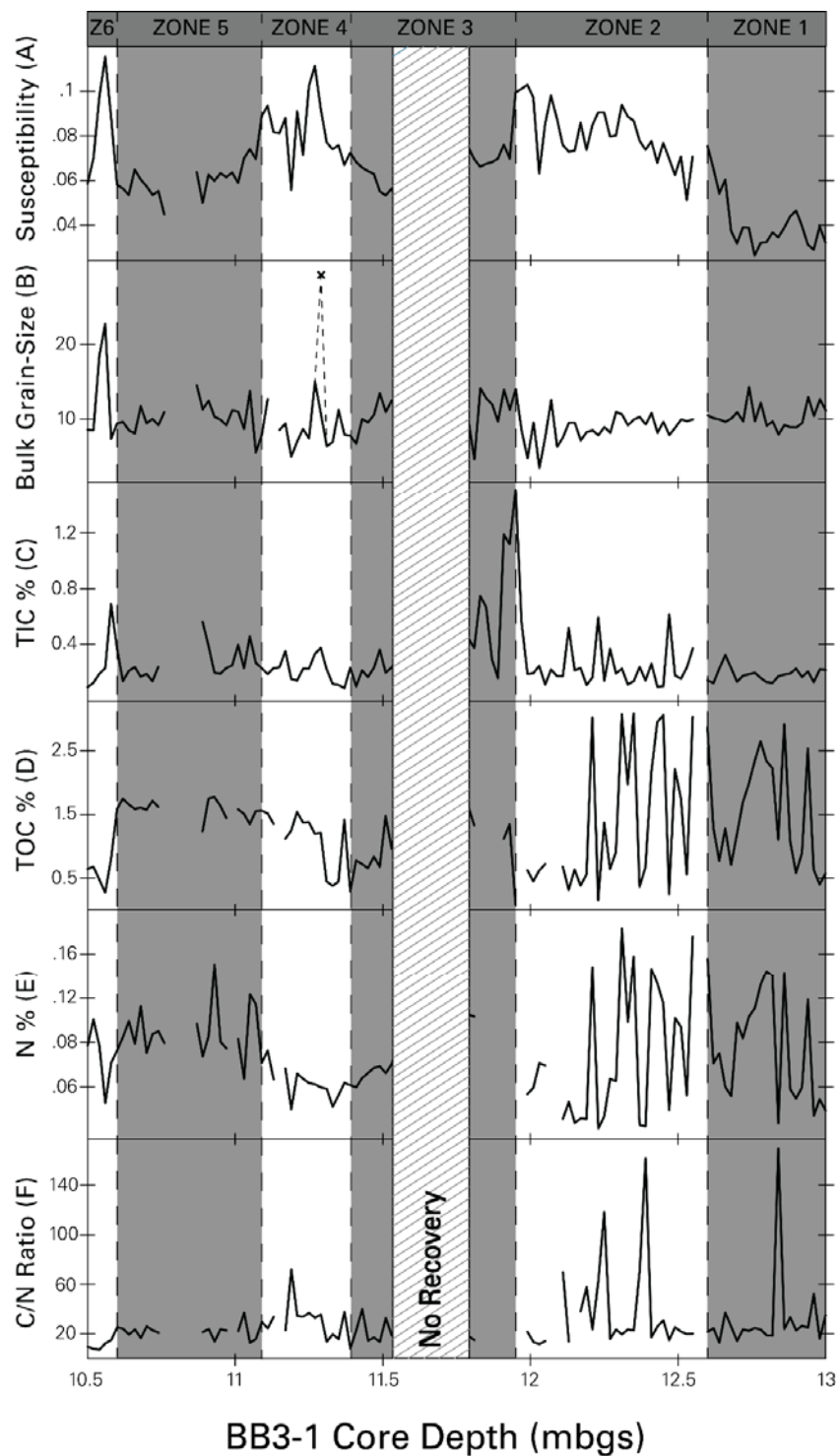


Figure 3. Geophysical and geochemical proxies from the BB3-I core. Zones 1-6 are defined by dashed lines. Gray backgrounds correspond to colder/drier climate while white backgrounds correspond to warmer/wetter climate as seen from pollen (Figure 1). Susceptibility = normalized magnetic susceptibility (κ), TIC = total inorganic carbon, TOC =

total organic carbon, N = nitrogen, C_{org}/N ratio = organic carbon nitrogen molar ratio. The x and dashed line within bulk grainsize represents an outlier value.

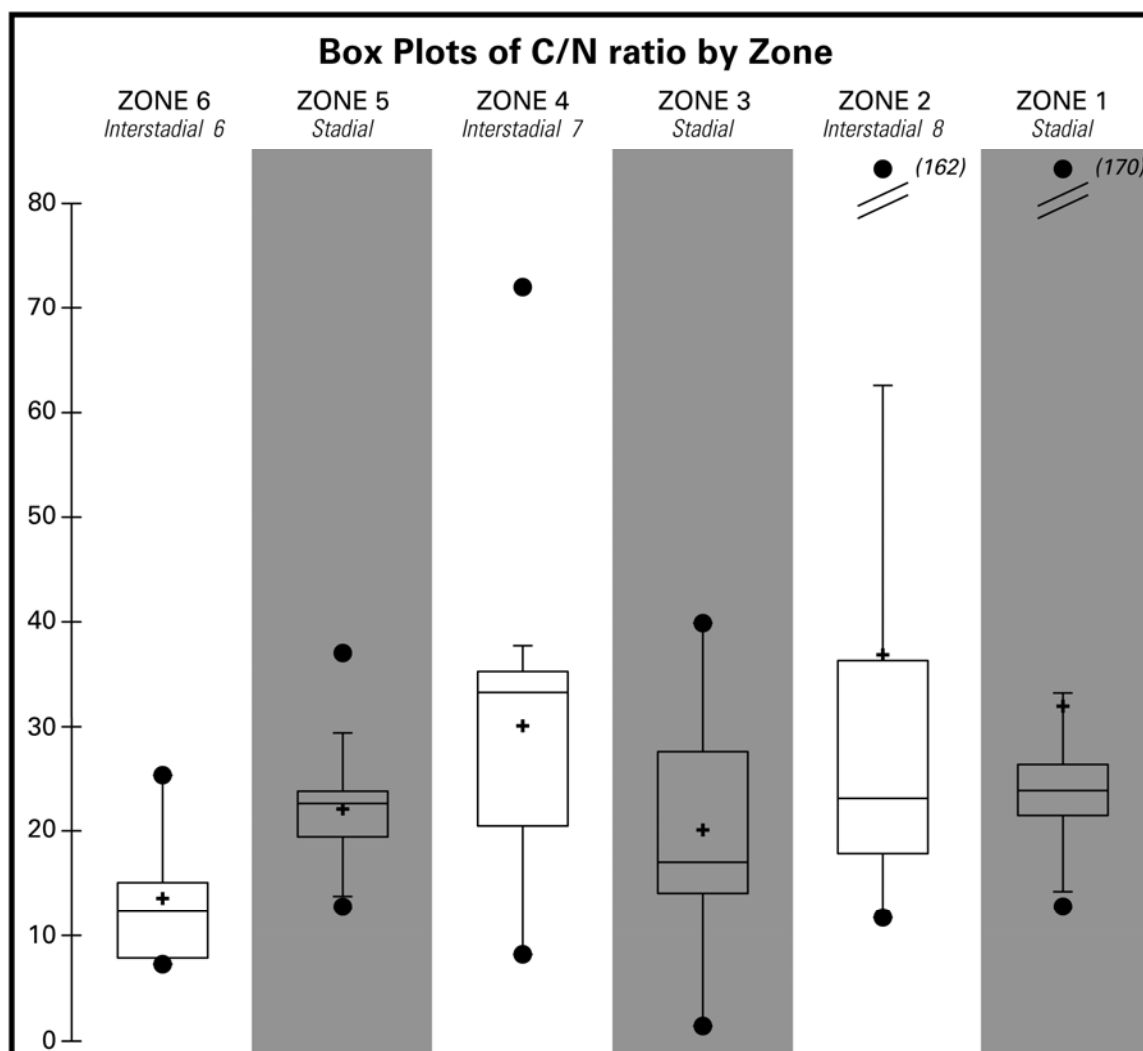


Figure 4. Box and Whisker Plot of C_{org}/N ratio. One box plot for each zone is displayed. The central horizontal lines denote medians. The lower and upper horizontal restraints of the box are the 1st and 3rd quartiles. All values above and below the whiskers are considered outliers. Black dots denote maximum and minimum values and crosses denote means. Shown are fluctuations between two types of zones characterized by relatively high and low C_{org}/N . Zones 1, 3, 5 and 6 are characterized as relatively low C_{org}/N values and zones 2 and 4 characterized as relatively high C_{org}/N . C_{org}/N is interpreted to have significance reflecting changes in the amount of water discharged into the lake.

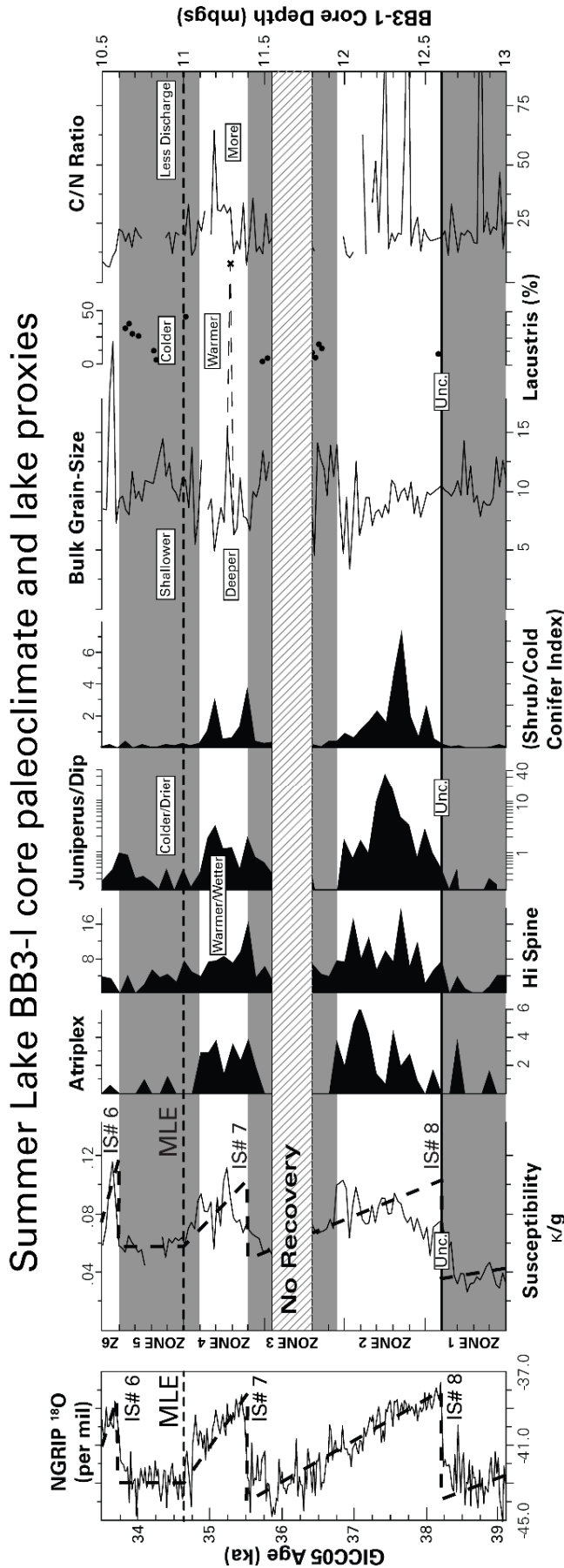


Figure 5. Correlation model of BB3-1 core with NGRIP ice core $\delta^{18}\text{O}$ data and locations of Dansgaard-Oeschger interstadial events (IS). NGRIP D-O interstadials are matched with the corresponding magnetic susceptibility highs from the BB3-1 core (shown in black dashed lines). Additional proxies of Atriplex, high spine concentrations, pollen ratios, bulk grain-size, *C. lacustris*, and C_{org}/N ratio represent lake temperature, regional temperature, precipitation, lake level and discharge into the lake. Shrub/Cold Conifer index consists of (Atriplex + Hi spine + Low spine + Rosaceae + Abies)/(Dip pine + Tsuga mertensiana + Picea + Sarcobatus). Gray backgrounds correspond to colder/drier climate, less discharge into the lake, colder lake temperature and shallower lake level. White backgrounds correspond to warmer/wetter climate, more discharge into the lake, warmer lake level and deeper lake level. The x and dashed line within bulk grainsize represent an outlier value.

References:

- Allison, I. S., 1982. Geology of Pluvial Lake Chewaucan, Lake County, Oregon: Corvallis, OR. Oregon State Univ. Press, vol. 11.
- Bachhubber, F.W., and Catto, N.R. 2000. Geologic evidence of rapid, multiple, and high-magnitude climate change during the last Glacial (Wisconsinian) of North America: Kluwer Academic Publishers. In: S.J. McLaren and D.R. Kniveton (eds.), Linking climate change to land surface change, pp. 143-169.
- Balch, D.P., Cohen, A.S., Schnurrenberger, D.W., Haskell, B.J., Valero-Garces, B.L., Beck, W.J., Cheng, H., and Edwards, L. 2005. Ecosystem and paleohydrological response to Quaternary climate change in the Bonneville Basin, Utah: *Paleogeography, Paleoclimatology, Paleoecology*, vol. 221, pp. 99-122.
- Baldwin, E. M., 1981. Geology of Oregon. Kendal/Hunt, Dubuque, Iowa: 170 pp.
- Benson, L.V., Burdett, J., Lund, S., Kashgarian, M., and Mensing, S., 1997. Nearly synchronous climate change in the Northern Hemisphere during the last glacial termination: *Nature*, vol. 388, pp. 263-265
- Benson, L., Lund S., Negrini, R.M., Linsley, B., and Zic, M., 2003. Response of North American Great Basin Lakes to Dansgaard-Oeschger oscillations: *Quaternary Science Reviews*, vol. 22, pp. 2239–2251.
- Benson, L., 2004. Western Lakes. The Quaternary Period in the United States-- Developments in Quaternary Science: Amsterdam, Elsevier. In: Gillespie, A.R., Porter, S.C., and Atwater, B., (eds.), p. 185-204.
- Benson, L.V., Lund, S.P., Smoot, J.P., Rhode, D.E., Spencer, R.J., Verosub, K.L., Louderback, L. A., Johnson, C.A., Rye, R.O., and Negrini, R.M., 2011. The rise and fall of Lake Bonneville between 45 and 10.5 ka: *Quaternary International*, vol. 235, pp. 57–69.
- Benson, L.V., Smoot, J.P., Lund, S.P., Mensing, S.A., Foit Jr., F.F., and Rye, R.O., 2012. Insights from a synthesis of old and new climate-proxy data from the Pyramid and Winnemucca lake basins for the period 48 to 11.5 cal ka: *Quaternary International*, vol. 310, pp. 62-82. doi:10.1016/j.quaint.2012.02.040.
- Blunt, A. B., and Negrini, R. M., 2015. Lake levels for the past 19,000 years from the TL05-4 cores, Tulare Lake, California, USA: Geophysical and geochemical proxies. *Quaternary International*, vol. 387, pp. 122-130.
- Bunbury, J. and Gajewski, K., 2009. Biogeography of freshwater ostracodes in the Canadian Artic Archipelago, Arctic, vol. 62(3), pp. 324-332.

- Carter, C., 1997. Ostracodes in core OL-92: Alternation of saline and freshwater forms through time. In G.I. Smith and J.L. Bischoff, editors, An 800,000-year paleoclimatic record from core OL-92, Owens Lake, Southeast California: Special Papers of the Geological Society of America, vol. 317, pp. 113-119.
- Cohen, A.S., Palacios-Fest, M.R., Negrini, R.M., Wigand, P.E., and Erbes, D.B., 2000. A paleoclimate record for the past 250,000 years from Summer Lake, Oregon, USA: II. Sedimentology, paleontology and geochemistry: *Journal of Paleolimnology*, vol. 24(2), pp. 151–182.
- Dansgaard, W., Johnsen, S. J., Clausen, H. B., Dahl-Jensen, D., Gundestrup, N. S., Hammer, C. U., ... and Bond, G., 1993. Evidence for general instability of past climate from a 250-kyr ice-core record: *Nature*, vol. 364(6434), pp. 218-220.
- Decrouy, L., Vennemann, T. W., and Ariztegui, D., 2012. Sediment penetration depths of epi-and infaunal ostracods from Lake Geneva (Switzerland): *Hydrobiologia*, vol. 688(1), pp. 5-23.
- Delorme, D.L., 1969. Ostracodes as Quaternary paleoecological indicators: *Canadian Journal of Earth Sciences*, vol. 6, pp. 1471-1476.
- Denniston R.F., Asmerom Y., Polyak V., Dorale J.A., Carpenter S.J., Trodick C., Hoye B. and Gonzalez L.A., 2007. Synchronous millennial-scale climatic changes in the Great Basin and the North Atlantic during the last interglacial: *Geology*, vol. 35, pp. 619-622.
- Donath, F. A., 1962. Analysis of Basin-Range structure, southcentral Oregon: *Geological Society of America Bulletin*, vol. 73, pp. 1–16.
- Donovan, L. A., Richards, J. H., and Muller, M. W., 1996. Water relations and leaf chemistry of *Chrysothamnus nauseosus* ssp. *consimilis* (Asteraceae) and *Sarcobatus vermiculatus* (Chenopodiaceae): *American Journal of Botany*, pp. 1637-1646.
- Forester, R.M., 1986. Determination of the dissolved anion composition of ancient lakes from fossil ostracodes: *Geology*, vol. 14, pp. 796-799.
- Grootes, P.M. and Stuiver, M., 1997. Oxygen 18/16 variability in Greenland snow and ice with 10–3- to 105-year time resolution: *Journal of Geophysical Research*, vol. 102, pp. 26455–26470.
- Hendy, I. L., and Kennett, J. P., 1999. Latest Quaternary North Pacific surface-water responses imply atmosphere-driven climate instability: *Geology*, vol. 27(4), pp. 291-294.

- Hunt, C.O., 1985. Recent advances in pollen extraction techniques: a brief review, in: N.R.J. Fieller, D.D. Gilbertson, N.G.A. Ralph (Eds.): *Palaeobiological Investigations*, British Archaeological Reports, vol. 266, pp. 181–187.
- Johnsen, S. J., Clausen, H. B., Dansgaard, W., Fuhrer, K., Gundestrup, N., Hammer, C. U., Iversen, P.L., Jouzel, J., Stauffer, B., and Steffensen, J. P., 1992. Irregular glacial interstadials recorded in a new Greenland ice core: *Nature*, vol. 359(6393), pp. 311-313.
- Kapp, R. O., Davis, O. K., and King, J. E., 2000. *Ronald O. Kapp's Pollen and Spores*. Second ed. College Station TX: The American Association of Stratigraphic Palynologists.
- Kirby, M.E., Zimmerman, S.R.H., Patterson, W.P., Rivera, J.J., 2012. A 9170-year record of decadal-to-multi-centennial scale pluvial episodes from the coastal Southwest United States: a role for atmospheric rivers: *Quaternary Science Reviews*, vol. 46, pp. 57-65.
- Kuehn, S. C., and Negrini, R. M., 2010. A 250 ky record of Cascade arc pyroclastic volcanism from late Pleistocene lacustrine sediments near Summer Lake, Oregon, USA: *Geosphere*, vol. 6(4), pp. 397-429.
- Laj, C., and Channell, J. E. T., 2007. Geomagnetic excursions: *Treatise on Geophysics*, vol. 5(373), pp. 416.
- Lanci, L., Kent, D. V., Biscaye, P. E., and Bory, A., 2001. Isothermal remanent magnetization of Greenland ice: Preliminary results: *Geophysical research letters*, vol. 28(8), pp. 1639-1642.
- Lister, K.H., 1975. Quaternary freshwater Ostracode from the Great Salt Lake Basin, Utah: *The University of Kansas Paleontological Contributions*, Paper 78.
- McCuan, D.T., 2011. Late Pleistocene Geomagnetic Field Recorded in Sediments from the Depocenter of Pluvial Lake Chewaucan, lake County, OR: A thesis submitted to the Department of Geological Sciences, California State University, Bakersfield.
- Medina, L.D. 2015, Carbon Geochemistry, Lithology, and Pollen from the TL05 Core and TL12 Outcrop, Tulare Lake, CA: *Lake Environmental Conditions*: A thesis submitted to the Department of Geological Sciences, California State University, Bakersfield.
- Mensing, S. A., Sharpe, S. E., Tunno, I., Sada, D. W., Thomas, J. M., Starratt, S., and Smith, J., 2013. The Late Holocene Dry Period: multiproxy evidence for an extended drought between 2800 and 1850 cal yr BP across the central Great Basin, USA: *Quaternary Science Reviews*, vol. 78, pp. 266-282.

- Meyers, P. A., & Ishiwatari, R., 1993. Lacustrine organic geochemistry—an overview of indicators of organic matter sources and diagenesis in lake sediments: *Organic geochemistry*, vol. 20(7), pp. 867-900.
- Meyers, P.A., and Doose, H., 1999. Sources, preservation, and thermal maturity of organic matter in Pliocene-Pleistocene organic-carbon-rich sediments of the western Mediterranean Sea. *Proc. ODP: Science Results*, vol. 161, pp. 383-390.
- Mifflin, M.D., and Wheat, M.M., 1979. Pluvial lakes and estimated pluvial climates of Nevada: *Nevada Bureau of Mines and Geology Bulletin*, University of Nevada, Reno. vol. 94, pp. 57
- Mikolajewicz, U., Crowley, T. J., Schiller, A., and Voss, R., 1997. Modelling teleconnections between the North Atlantic and North Pacific during the Younger Dryas: *Nature*, vol. 387(6631), pp. 384-387.
- Moore, P. D., and Webb, J. A. 1978: *Illustrated guide to pollen analysis*. Hodder and Stoughton.
- Negrini, R. M., J. O. Davis and K. L. Verosub, 1984. Mono Lake geomagnetic excursion found at Summer Lake, Oregon: *Geology*, vol. 12, pp. 643–646.
- Negrini, R. M., Erbes, D., Faber, K., Herrera, A., Roberts, A., Cohen, A. and Foit, F., 2000. A paleoclimate record for the past 250,000 years from Summer Lake, Oregon, USA. 1. Chronology and magnetic proxies for lake level: *Journal Paleolimnology*, vol. 24, pp. 125–149, doi:10.1023/A:1008144025492.
- Negrini, R. M., McCuan, D.T., Horton, R.A., Lopez, J.D., Cassata, W.S., Channell, J.E., Verosub, K.L., Knott, J.R., Coe, R.S., Liddicoat, J.C., Lund, S.P., Benson, L.V., and Sarna-Wojcicki, A.M., 2014. Nongeocentric axial dipole field behavior during the Mono Lake excursion. *Journal Geophysical Research: Solid Earth*, vol. 119, pp. 2567-2581. doi:10.1002/2013JB010846.
- Oster, J.L., Montañez, I.P., Mertz-Kraus, R., Sharp, W.D., Stock, G.M., Spero, J.J., Tinsley, J., and Zachos, C., 2014. Millennial-Scale Variations in Western Sierra Nevada Precipitation during the last glacial cycle MIS 4/3 Transition: *Quaternary Research*, vol. 82, pp. 236-248.
- Oster, J. L., Ibarra, D. E., Winnick, M. J., and Maher, K., 2015. Steering of westerly storms over western North America at the Last Glacial Maximum: *Nature Geoscience*, vol. 8(3), pp. 201-205.
- Oviatt, C.G., Thompson, R.S., Kauffman, D.S., Bright, J., and Forester, R.M., 1999. Reinterpretation of the Burmester core, Bonneville basin, Utah: *Quaternary Research*, vol. 52(2), pp. 180-184.

- Palacios-Fest, M. R., Cohen, A. S., Ruiz, J., and Blank, B., 1993. Comparative paleoclimatic interpretations from nonmarine ostracodes using faunal assemblages, trace elements shell chemistry and stable isotope data: *Geophysical Monograph-American Geophysical Union*, vol. 78, pp. 179-179.
- Reheis, M. C., Adams, K. D., Oviatt, C. G., and Bacon, S. N., 2014. Pluvial lakes in the Great Basin of the western United States—a view from the outcrop: *Quaternary Science Reviews*, vol. 97, pp. 33-57.
- Sperazza, M., Moore, J.M., Hendrix, M.S., 2004. High-Resolution Particle Size Analysis of Naturally Occurring Very Fine-Grained Sediment Through Laser Diffractometry: *Research Methods Paper: Journal of Sedimentary Research*. vol. 74(5), pp. 736-743
- Smith, R. J., and Janz, H. 2008. Recent species of the family Candonidae (Ostracoda, Crustacea) from the ancient Lake Biwa, central Japan: *Journal of Natural History*, vol. 42(45-46), pp. 2865-2922.
- Snowball, I. F. 1993. Geochemical control of magnetite dissolution in subarctic lake sediments and the implications for environmental magnetism: *Journal of Quaternary Science*, vol. 8(4), pp. 339-346.
- Svensson, A., Anderen, K. K., Bigler, M., Clausen, H.B., Dahl-Jensen, D., Davies, S.M., Johnsen, S.J., Muscheler, R., Parrenin, F., Rasmussen, S. O., Rothlisberger, R., Seierstad, I., Steffensen, J.P., and Vinther, B. M., 2008. A 60,000 year Greenland stratigraphic ice core chronology: *Climate of the Past*, vol. 4, pp. 47–57, doi:10.5194/cp-4-47-2008.
- Thompson, R. S., Anderson, K. H., and Bartlein, P. J., 1999. Atlas of relations between climatic parameters and distributions of important trees and shrubs in North America: US Department of the Interior, US Geological Survey.
- Wagner, G., Beer, J., Laj, C., Kissel, C., Masarik, J., Muscheler, R., and Synal, H. A., 2000. Chlorine-36 evidence for the Mono Lake event in the Summit GRIP ice core: *Earth and Planetary Science Letters*, vol. 181(1), pp. 1-6. doi:10.1016/S0012-821X(00)00196-5. Walker 1969
- Walker, G. W., 1969. Geology of the High Lava Plains province: Oregon Dept. Geol. Min. Ind. Bull. 64: 77–79.
- Walker, G. W., and MacLeod, N.S., 1991. Geologic map of Oregon, scale 1:500,000: U.S. Geol. Surv.
- Wigand, P. E., and Rhode, D., 2002. Great Basin vegetation history and aquatic systems: the last 150,000 years. *Great Basin aquatic systems history*. Washington, DC, USA: Smithsonian Institution Press, *Smithsonian contributions to earth sciences*, vol. 33, pp. 309-367.

Wise, E. K., 2010. Spatiotemporal variability of the precipitation dipole transition zone in the western United States: *Geophysical Research Letters*, vol. 37(7).

Zic, M., Negrini, R.M., and Wigand, P.E., 2002. Evidence of synchronous climate change across the Northern Hemisphere between the North Atlantic and the northwestern Great Basin, United States: *Geology*, vol. 30, pp. 635–638, doi:10.1130/0091-7613(2002)030<0635:EOSCCA>2.0.CO;2.